

DOI: 10.5281/zenodo.12426678

"DYNAMIC SPECTRUM-AWARE CSS FRAMEWORK USING HYBRID FCK-MEANS CLUSTERING WITH ADAPTIVE CENSORING AND MULTI-ANTENNA FUSION UNDER FADING CONDITIONS"

V. Parimala^{1*}, K. Devarajan²

¹Department of Electronics and Communication, Chennai Institute of Technology, Tamil Nadu, India.
Email: itsmepari@gmail.com

²Department of Electronics and Communication, Annamalai University, Tamil Nadu, India
Email: devarajan_lecturer@yahoo.com

Received: 25/12/2025
Accepted: 20/01/2026

Corresponding Author: V. Parimala
(itsmepari@gmail.com)

ABSTRACT

Cognitive radio networks (CRNs) enable opportunistic spectrum access through Cooperative Spectrum Sensing (CSS), wherein Secondary Users (SUs) identify spectrum holes without interfering with Primary Users (PUs). This paper presents a dynamic spectrum-aware CSS framework that integrates a hybrid FCK-Means clustering algorithm with adaptive censoring and multi-antenna decision fusion under diverse fading environments. The model accounts for real-time SNR variations and interference-induced signal distortion, offering adaptive thresholding and noise-resilient classification for reliable PU detection. A two-stage clustering process—combining Fuzzy C-Means and K-Means—minimizes false alarms while enhancing classification under non-convex and noisy conditions. Each SU processes local decisions using Selection Decision (SD) merging logic, and decisions are fused at the Fusion Center (FC) using Maximal Ratio Combining (MRC), guided by optimized SNR-based censoring thresholds. The framework is benchmarked across Rayleigh, Nakagami, and Rician fading channels, quantifying trade-offs in energy consumption, detection probability, sensing time, and spectrum utilization. Comparative evaluations against CNN and RNN-based spectrum sensing highlight the proposed model's computational efficiency. Experimental results demonstrate improved accuracy, recall, and reduced false alarm rates, establishing the robustness and adaptability of the hybrid FCK-Means model under fluctuating PU activity and high-interference scenarios.

KEYWORDS: Cooperative Spectrum Sensing; FCK-Means; Multiple Antennas; Censoring-oriented concept; Fading Channels; Primary User; Secondary User.

I. INTRODUCTION

The exponential growth of wireless services and smart applications has led to intense competition over the finite radio spectrum, intensifying the need for more intelligent and dynamic spectrum utilization strategies. **Cognitive Radio (CR)** technology, initially proposed by Mitola and Maguire [11] and further developed by Haykin [12], offers a paradigm shift that enables unlicensed Secondary Users (SUs) to opportunistically access underutilized spectrum without interfering with Primary Users (PUs). This dynamic access is achieved through continuous spectrum sensing, adaptation, and decision-making mechanisms [1].

At the core of CR functionality lies **spectrum sensing**, the process of detecting spectrum holes where PUs are inactive. However, individual sensing at a single SU is often unreliable due to noise, multipath fading, and shadowing. To enhance detection accuracy, **Cooperative Spectrum Sensing (CSS)** has been introduced, allowing multiple SUs to share their local observations to make a more robust global decision at the Fusion Center (FC) [14], [20]. While CSS improves sensing reliability, it also introduces new challenges, including increased signaling overhead, higher latency, and elevated energy consumption—particularly in multi-hop and large-scale networks [2], [13].

Energy-efficient spectrum sensing has thus become a central research focus in modern CRNs. Several models have been proposed to balance sensing accuracy and energy usage. For example, Arienzo and Tarchi [2] modeled energy trade-offs in multi-hop networks, while Sun et al. [6] highlighted the need to balance spectrum opportunity utilization and power efficiency. However, many traditional approaches rely on static or rigid frameworks, which fail to adapt to real-time PU dynamics, SNR fluctuations, or interference variability [3], [17].

To address network scalability and reporting efficiency, **clustering techniques** have been widely adopted. In this structure, SUs are grouped into clusters, each managed by a **Cluster Head (CH)** responsible for aggregating local sensing data and forwarding it to the FC [9], [10]. Cluster formation is influenced by geographic location, signal quality (SNR), node energy levels, and channel availability [22]. Yet, in dynamic environments, static clustering and hard-decision rules often result in **elevated false alarm rates and misclassification**, particularly under fading conditions and noisy settings [5], [16].

In light of these challenges, we propose an advanced CSS framework using a **Modified Fuzzy C-Means and K-Means (FCK-Means)** hybrid

clustering algorithm. This approach leverages the soft classification capability of FCM to manage ambiguity in spectrum data and combines it with K-Means for precise boundary detection, improving robustness against noise and non-convex data patterns [21]. Compared to deep learning models such as CNNs and RNNs—which require large datasets and high computational power—the proposed hybrid method is unsupervised, lightweight, and adaptable to changing spectrum conditions [1], [4].

Our model enhances local SU decisions by employing multiple antennas for spatial diversity, thereby capturing more reliable signal features. Adaptive censoring is then applied based on real-time SNR thresholds to filter out unreliable or energy-inefficient SUs, reducing unnecessary reporting [15], [8]. Final decisions at the FC are refined using **Maximal Ratio Combining (MRC)**, which weights SU inputs according to their channel quality, leading to enhanced global decision performance [7].

The framework also addresses **cross-layer interference**, dynamic spectrum access, and fading variability by enabling dynamic re-clustering and parameter adjustment based on ongoing network feedback [24], [25]. It supports operation under diverse fading scenarios—**Rayleigh, Nakagami, and Rician**—ensuring adaptability and resilience in both urban and high-mobility environments [18], [19].

This study evaluates the proposed method using comprehensive metrics, including detection probability, false alarm rate, energy consumption, classification accuracy, sensing time, and throughput. Comparative analysis with both clustering and deep learning benchmarks reveals superior performance and lower complexity. The results highlight the **scalability, efficiency, and robustness** of the proposed framework in modern cognitive radio environments [6], [26].

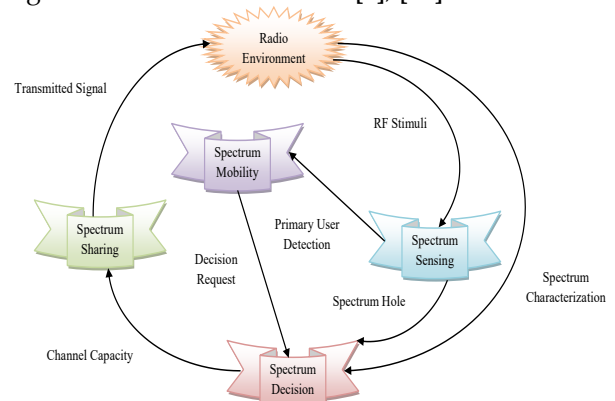


Fig. 1. *Cognitive Cycle Illustration*
The paper contribution is.

Performance Evaluation of CSS Under Noisy and Fading Conditions:

A detailed performance analysis of CSS is conducted under diverse channel models—**Rayleigh, Nakagami, and Rician fading**—to assess detection accuracy, false alarm rate, sensing time, and energy consumption. The study explicitly examines **noise-induced variations, SNR fluctuations**, and their impact on misclassification in dynamic PU environments.

Development of a Hybrid FCK-Means Clustering-Based Detection Mechanism:

A novel two-stage clustering approach, **FCK-Means**, is introduced. It combines **Fuzzy C-Means (FCM)** for soft clustering and **K-Means** for boundary refinement. This hybrid model enhances classification accuracy, reduces false alarms, and improves adaptability under **non-convex** and **high-interference** data distributions. The model also demonstrates computational efficiency when compared to deep learning alternatives such as CNNs and RNNs.

Integration of Multi-Antenna Spectrum Sensing with Adaptive Selection Decision (SD):

Each Secondary User (SU) is equipped with multiple antennas and applies FCK-Means to sense PU activity. The **Selection Decision (SD)** logic merges antenna-based outputs adaptively based on local SNR conditions, improving detection reliability and suppressing erratic inputs due to channel impairments or cross-layer interference.

Censoring-Based Fusion Decision (FD) with Maximal Ratio Combining (MRC):

A **censoring mechanism based on real-time SNR estimation** is employed at the Fusion Center (FC) to filter unreliable SU reports, reducing communication overhead and enhancing energy efficiency. The remaining decisions are fused using **Maximal Ratio Combining (MRC)** to provide a robust global decision that accounts for the **weight and reliability** of each SU's report.

Optimization of Censoring Thresholds and Algorithm Parameters:

A mathematical framework is presented to derive the **optimal censoring thresholds** under dynamic SNR and fading conditions. The parameters of the FCK-Means model are also fine-tuned to improve detection robustness, minimize miss detection rates, and balance spectrum utilization and energy constraints across different network scenarios.

Validation of Spectrum Utilization and Clustering Scalability:

The proposed method includes an evaluation of how **SU clustering and cluster head selection** affect global detection accuracy and computational load at the FC. The results demonstrate that adaptive clustering strategies can maintain high sensing performance even under growing SU densities and varying interference levels.

The paper organization is. Section I shows the CSS introduction. The literature works are in Section II. Section III gives the system model and energy efficiency of CSS. The proposed system model of CRNs is explained in Section IV. Section V describes the fusion rule of the suggested CSS model. The results are shown in Section VI. Conclusion is in Section VII.

II. LITERATURE SURVEY

A. Related Works

In 2020, Cai and Zhang [1] have suggested a combined optimization method for dynamic spectrum access and coding that was performed by reinforcement learning, and the program's performance was tested through simulations, resulting in a viable research avenue for the implementation of cognitive spectrum cooperation.

In 2015, Arienzo and Tarchi [2] have labelled the statistical modelling of spectrum sensing energy usage in CRNs. For the simulation of interference in CRNs, a Poisson point process has been demonstrated to produce tractable and appropriate outcomes. We used this homogeneous stochastic technique to create a unified model for calculating spectrum sensing energy consumption in clustered CRNs. We also expanded the architecture to include multi-hop networks. As a function of the count of secondary users, their spatial density, and the count of hops in the CRN, the spectrum sensing energy may be described as a Gamma-truncated distribution, according to the letter.

In 2016, Düzenli and Akay [3] have suggested a novel dynamic spectrum sensing technique for primary users (PUs), where at least one and perhaps many PU status modifications are envisaged to happen in the channel during the sensing time. The latest status change point of the PU is calculated initially, on the basis of the suggested technique, utilising maximum likelihood estimation (MLE). The observed samples can then be subjected to any known spectrum sensing technique among this final status change point and the conclusion of the sensing time. As a result, the likelihood of detection is

reduced as a result of PU traffic. The MLE computation is sped up via dynamic programming (DP). A novel cumulative sum (CuSum)-oriented weighting technique was also proposed. Simulations showed that the suggested sensing technique improved the likelihood of detection for the entire spectrum sensing techniques investigated. Moreover, when combined with the latest status change point estimate technique, the suggested CuSum-based weighting system obtained the highest chance of detection.

In 2014, Hattab and Ibnkahla [4] have presented an in-depth examination of current advances in multiband spectrum sensing methods, as well as their limits and potential future prospects for improvement. To address a basic constraint on diversity and sampling, we investigated cooperative communications for MB-CRNs. We also looked at the constraints and tradeoffs of different MB-CRN design factors. Additionally, we looked at the main performance measures for MB-CRNs that were different from those utilized for single-band networks.

In 2015, Li *et al.* [5] have regarded a wideband CRN that could simultaneously sense multiple narrowband channels and therefore accumulated the identified channels available for transmission, and introduced a new CR model that has enhanced sensing throughput and could reduce secondary user (SU) power consumption differentiated with the traditional CR model studied so far. We investigated the conflict of modeling the "optimal sensing time and power allocation strategy" for the suggested CR model in order to maximize the ergodic throughput under two distinct strategies, such as the "wideband sensing-oriented spectrum sharing scheme and the wideband opportunistic spectrum access scheme", in the recommended CR model. A sub gradient technique was designed to achieve the ideal sensing time and the appropriate power allocation approach for the two strategies, in addition to the average interference power restriction at main user. Furthermore, numerical simulations were shown to demonstrate the effectiveness of the two strategies offered.

In 2016, Sun *et al.* [6] have investigated the tradeoff among "spectrum sensing performance and spectrum opportunity" usage in the CR network. We used mathematics to solve the tradeoff issue. The best tradeoff was mostly determined by the principal user's activities. On the basis of the technique of the presented tradeoff issue, CSS was also investigated. To evaluate the influence of distinct factors on the optimum spectrum sensing time, we used numerical analysis.

In 2015, Tadayon and Aissa [7] have suggested a multichannel learning-oriented distributed sensing fusion (MC-LDS) method for WRANs as a distributed spectrum sensing approach. The intrinsic reward-penalty strategy of MC-LDS has been shown to be self-trained, stable, and to adjust for defect reporting. MC-LDS was also more consistent in the entire traffic regimes, was fair, customizable, and bandwidth effective. The findings of simulations and comparisons showed that MC-LDS outperformed the IEEE 802.22 suggested algorithms, namely the "AND, OR, and VOTING rules".

In 2014, Althunibat and Granelli [8] have developed a new CSS system that was more energy efficient. According to the suggested approach, just a single CU would broadcast its local decision to the entire network. The remaining CUs having a distinct local decision would object to the fusion centre, while those that agree with the declared decision would remain silent. As a result, the fusion centre would be aware of the entire CUs' local decisions before making a global decision. An analytical analysis was offered on how to pick the broadcasting CU in order to enhance energy effectiveness. In comparison to the literature, simulation as well as analytical findings investigated the energy efficiency increase.

In 2017, Sharma *et al.* [9] have reviewed various clustering strategies, investigate their performances, and also learnt their performance regarding the clustering mechanism in CRN.

In 2014, Lim *et al.* [10] have shown clustering algorithms being defined by clustering aims, metrics, and the count of hops in every cluster, among other things. We also discussed complexity analyses, performance improvements made by clustering algorithms, and outstanding concerns in order to lay the groundwork for future study and pique fresh research interests in this field.

B. Review

Cognitive technology can be utilized for spectrum sensing and availability in a future scenario where everything is attached, and emerging coding techniques can be employed to confront packet erasure created by dynamic spectrum access and realize cognitive spectrum collaboration within the users in mass connection situations. In the deployment of smart networks, machine learning approaches are becoming more popular. Table I lists the features and challenges of existing cognitive radio spectrum sensing methods. Reinforcement learning [1] minimizes the convergence speed and also verifies the scalability. But, the packet transmitting scheme and the optimal coding structure is not attained. Gamma distribution [2] enhances the

sensing energy with growing network hop count and also optimizes the consumption of energy. Still, the activity of the licensed users is not considered. Change point estimation [3] offers a noticeable enhancement noticeable enhancement with respect to the detection probability and also eradicates the disturbing effect associated with the noise only samples. Yet, it does not properly minimize the system overhead. Design tradeoff [4] improves the bandwidth efficiency and a desirable compromise is offered among the sampling complexity and spatial diversity. But, it does not minimize the needed sensing duration. Wideband spectrum sensing [5] saves the power and also enhance the throughput. Still, it does not consider multiple primary users. Spectrum opportunity [6] mathematically analyzes the tradeoff problem and also minimizes the optimal sensing time. Yet, the

opportunities are given to unlicensed users in rare cases. MC-LDS [7] supports the spectrum databases by the spectrum sensing information and the cognitive systems are stabilized to enhance the performance. But, it purely relies on the sensing outcomes. CSS [8] does not degrade the global achievable throughput and the overall detection accuracy is not affected. Still, the FC does not make the broadcasted decision by itself. IoT [9] is applicable for the CR network application and the resource needs are minimized. Yet, it is critical to the NGN realization. Optimization [10] attains better tradeoff among communication overhead and sensing efficiency and the comparable performance is reaped with the authentication mechanism. But, the malicious user count is increased. Thus, it is needed to suggest novel techniques for the cognitive radio spectrum sensing methods.

TABLE I. FEATURES AND CHALLENGES OF TRADITIONAL COGNITIVE RADIO SPECTRUM SENSING METHODS.

Author [citation]	Methodology	Features	Challenges
Cai and Zhang [1]	Reinforcement learning	<ul style="list-style-type: none"> The scalability is verified. It minimizes the convergence speed. 	<ul style="list-style-type: none"> It does not attain the packet transmitting scheme and the optimal coding structure.
Arienzo and Tarchi [2]	Gamma distribution	<ul style="list-style-type: none"> The consumption of energy is optimized. The sensing energy is enhanced with growing network hop count. 	<ul style="list-style-type: none"> It does not consider the activity of the licensed users.
Düzenli and Akay [3]	Change point estimation	<ul style="list-style-type: none"> The disturbing effect associated with the noise only samples are eradicated. A noticeable enhancement is offered with respect to the detection probability. 	<ul style="list-style-type: none"> The system overhead is not minimized properly.
Hattab and Ibnkahla [4]	Design tradeoff	<ul style="list-style-type: none"> A desirable compromise is offered among the sampling complexity and spatial diversity. The bandwidth efficiency is improved. 	<ul style="list-style-type: none"> It does not minimize the needed sensing duration.
Li <i>et al.</i> [5]	Wideband spectrum sensing	<ul style="list-style-type: none"> The throughput is enhanced. The power is saved. 	<ul style="list-style-type: none"> Multiple primary users are not considered.
Sun <i>et al.</i> [6]	Spectrum opportunity	<ul style="list-style-type: none"> It minimizes the optimal sensing time. The tradeoff problem is mathematically analyzed. 	<ul style="list-style-type: none"> The opportunities are given to unlicensed users in rare cases.
Tadayon and Aissa [7]	MC-LDS	<ul style="list-style-type: none"> The cognitive systems are stabilized to enhance the performance. The spectrum databases are supported by the spectrum sensing information. 	<ul style="list-style-type: none"> It purely relies on the sensing outcomes.
Althunibat and Graneli [8]	CSS	<ul style="list-style-type: none"> The overall detection accuracy is not affected. The global achievable throughput is not degraded. 	<ul style="list-style-type: none"> The FC does not make the broadcasted decision by itself.
Sharma <i>et al.</i> [9]	Clustering	<ul style="list-style-type: none"> The clustering process returns better outcomes. It reveals high accuracy. 	<ul style="list-style-type: none"> It fails to make self decisions in rare cases.
Lim <i>et al.</i> [10]	Clustering	<ul style="list-style-type: none"> The performance is better when compared with others. 	<ul style="list-style-type: none"> More optimization techniques can be included.

III. SYSTEM MODEL OF CSS

A. System Model

The main aim of this work is to detect whether primary user is present or not through the introduction of clustering concept. License will be

provided only to the primary users and it will not be given to the secondary users. The secondary users are subjected inside the clustering process using the FCK-Means that detects whether primary user is present or not. The selection combiner is used to select which output from the antenna is best. This is

achieved by selecting the antenna having least noise. From this, the data is sent to the fusion centre. Finally, the majority logic detects whether the primary user is present or not.

Fig. 2 depicts the suggested system methodology. "1000 *SUs* and three *PUs*" make up this system. The *PU*, as well as *FD* (Fusion Decision), is assumed to have a single transmit/receive antenna, while every *SU* has *N* receive antennas, an *FCK*-Means, and a single transmit antenna. The channel between the *PU* and the *SU* is said to be *S*-Channel or Sensing Channel and the channel between the *SU* and *FD* is called *R*-Channel or Reporting Channel. The *R*-channel is used by the entire *SUs* to send their sensing data to the *FD*. Every *SU* is grouped into clusters using the *FCK*-Means algorithm and receives signals from its *N* antennas and analyses them with the *FCK*-Means assigned to it and decides whether *PU* is present or absent. The output of each cluster is given to *SD* (Selection Decision). The *SD* is used to integrate the output of each cluster in the *S*-Channel and reach a local decision. The output of *SD* is fed to the *FD*. As the present system model is tested under different fading environment, we consider that both *R*-Channel and *S*-Channel is affected by fading ("(i) noisy-Rayleigh faded; (ii) noisy-nakagami faded; and (iii) noisy-Rician faded"). A binary decision is used to send the sensed data through the *R*-Channel. The decision of the *SUs* will be affected due to the presence of fading in the channel as the *SUs* are located far from the *FD*. So the *SUs* who have experienced fading or shadowing is stopped from transmitting their decision to the *FD*. This censoring of *SU* is done by calculating the *SNR* of each channel (the entire *SUs* are considered to contain a similar value of λ). The *SD* whose *SNR* is high is allowed to transmit while the other *SDs* are censored from transmitting their decisions. This will limit the energy consumption of the system and also save the transmission band for other *SU* transmissions. This censoring will further reduce the error rate (false alarm probability and miss detection probability) and improve the sensing time of the system. The *FD* employs Maximum Ratio Combined (*MRC*) to improve the accuracy of detection probability and increase the spectrum utilization of the system. The *FD* will make a global decision as to whether the *PU* is present or absent H_0 and H_1 . At every *SU*, the received signal at the j^{th} antenna $j = 1, 2, \dots, N$ may be represented as follows in Eq. (1).

$$z_j(o) = \begin{cases} o_j(o) & H_0 \\ i_j t(o) + o_j(o) & H_1 \end{cases} \quad (1)$$

In the above equation, an unknown signal

from *PU* having energy F_t is $\{o_j(o)\}_{j=1}^N$ represents the independent as well as identically distributed (i.i.d) zero-mean circularly symmetric complex Gaussian random variables, i.e., $o_j(o) \sim \zeta N(0, \sigma_o^2)$, in which σ_o^2 describes the noise variance; i_j shows the *S*-channel fading coefficient at the j^{th} antenna at every *SU*, also modelled as circularly symmetric complex Gaussian, with both mean as well as variance based on the format and the hypotheses related with the *PU*s presence or absence is H_1 and H_0 . We presume that $\{i_j\}$ are self-contained. The X_j decision variable at every *SU*'s j^{th} antenna for determining the presence or absence of the *PU* is in Eq. (2).

$$X_j = |z_j|^q \quad (2)$$

The *FCK*-Means parameter is $q > 0$ in this case. For $q = 2$, it can be shown from Eq. (2) that X_j decreases to the decision variable. It gives the generic equations for the false alarm as well as the miss detection probabilities as follow in Eq. (3) and Eq. (4).

$$Q_g = \int_{\lambda}^{\infty} f_{a|H_0}(a) da = 1 - F_{A|H_0}(\lambda); \quad A \geq 0 \quad (3)$$

$$Q_n = \int_0^{\lambda} f_{a|H_1}(a) da = F_{A|H_1}(\lambda); \quad A \geq 0 \quad (4)$$

Under hypotheses H_0 and H_1 , the conditional probability density functions (*PDFs*) of the choice variable $f_{a|H_k}$ are $f_{a|H_0}$ and s , accordingly. At every antenna, the cumulative distribution function (*CDF*) may be represented as in Eq. (5).

$$F_{X_j|H_k}(y) = Qs[|z_j|^q |_{H_k} \leq y]_{k=0,1} \quad (5)$$

Probability is denoted by $Qs[\cdot]$. Every *SU* assesses its decision variables (i.e., $\{X_j\}_{j=1}^N$) for the entire *N* antennas and employs the *SU* diversity approach, which produces the maximum value from *N* decision variables assessed for distinct diversity branches, i.e., $A = \max\{X_1, X_2, \dots, X_N\}$. Under hypothesis H_0 , the conditional *CDF* with *SD* is provided by Eq. (6).

$$F_{A|H_0}(a) = \left[1 - \exp\left(-\frac{a^{2/q}}{\sigma_o^2}\right) \right]^N \quad (6)$$

The *SDs* output is now subjected to a binary hard detector, which makes the following judgement on the presence or absence of a *PU* as in Eq. (7).

$$\begin{matrix} 1 \\ A > \lambda \\ < \\ 0 \end{matrix} \quad (7)$$

If λ_o defines the normalized detection threshold (to be calculated) and σ_o shows the noise standard deviation, then the detection threshold λ at an *SU* may be represented as $\lambda = \lambda_o \sigma_o^q$. The Fuzzy-K-Means (power *q* operation) of the entire *SUs* is considered to

be the same, as is the detection threshold. Following, the λ_o is determined by normalizing λ with a factor affecting q . The false alarm probability Q_f at an SU may be calculated using Eq. (3), Eq. (6), and Eq. (7).

$$Q_f = 1 - \left[1 - \exp\left(-\frac{\lambda^{2/q}}{\sigma_o^2}\right) \right]^N \tag{8}$$

We note that Q_f is similar in every fading scenario since there exists no PU signal under H_0 . As a result, it will not be explored anymore.

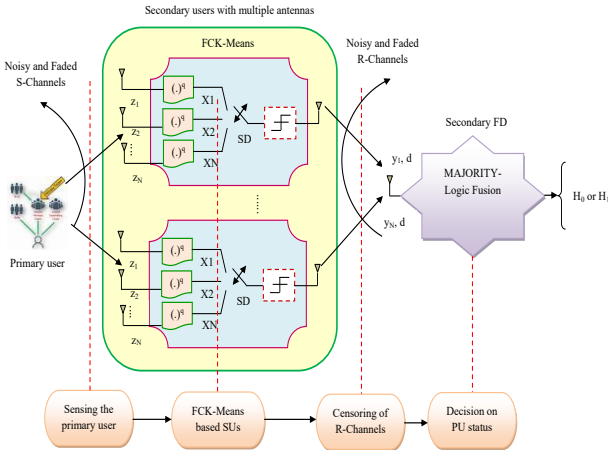


Fig. 2. System model of CSS

B. Rayleigh Faded Environment

Every channel gain i_j describes a circularly symmetric zero mean complex Gaussian random variable having variance σ_i^2 here, i.e. $i_j \sim \mathcal{CN}(0, \sigma_i^2)$. The likelihood of missing a target may be stated as in Eq. (9).

$$Q_n^{Sb} = \left[1 - \exp\left(-\frac{\lambda^{2/q}}{\sigma_o^2(1+\bar{\gamma}_t)}\right) \right]^N \tag{9}$$

In the above equation, the connection within a PU and an SU has an average SNR of $\bar{\gamma}_t = F_t \sigma_i^2 / \sigma_o^2$. The optimal detection threshold (signified as λ_{opt}) is derived by combining Eq. (9) and Eq. (10), i.e., the threshold where the overall error rate ($Q_n^{Sb} + Q_g$) of a single SU is minimised. For λ_{opt} constant values of q and $\bar{\gamma}_t$, a first order partial derivative of $Q_n^{Sb} + Q_g$ with respect to λ is computed and the outcome is placed to zero, i.e., $\partial(Q_n^{Sb} + Q_g) / \partial \lambda = 0$. It should be mentioned that tracking a general case of N antennas mathematically λ_{opt} is challenging. Yet, for $N = 1$ and $N = 3$, the following closed-form expressions of λ_{opt} may be achieved: $[\sigma_o^2(1 + \bar{\gamma}_t) \ln(1 + \bar{\gamma}_t) / \bar{\gamma}_t]^{q/2}$ and $[\sigma_o^2(1 + \bar{\gamma}_t) \ln(1 + \bar{\gamma}_t) / 2\bar{\gamma}_t]^{q/2}$ (10)

C. Hoyt or Nakagami-q Fading Environment

The fading coefficient at the j^{th} antenna i_j ($j = 1, \dots, N$) may be described as a complex nakagami

random variable in this environment. Following hypothesis H_1 , the conditional PDF of X_j can be generated with the use of a correct random variable transformation as follow in Eq. (11).

$$f_{X_j|H_1}^{H_0}(z) = \frac{z^{\frac{2}{q}-1}}{q\sigma_1\sigma_2} \exp\left[-\frac{z^{\frac{2}{q}}}{4}\left(\frac{1}{\sigma_1^2} + \frac{1}{\sigma_2^2}\right)\right] \times J_0\left[\frac{z^{\frac{2}{q}}}{4}\left(\frac{1}{\sigma_2^2} - \frac{1}{\sigma_1^2}\right)\right]; \quad j = 1, \dots, N \tag{11}$$

Here, $\sigma_1^2 = F_t \sigma_{i1}^2 + \sigma_o^2 / 2$; $\sigma_{i1} = \sqrt{\Omega r^2 / 1 + r^2}$; $\sigma_2^2 = F_t \sigma_{i2}^2 + \sigma_o^2 / 2$; $\sigma_{i2} = \sqrt{\Omega / 1 + r^2}$; the average fading power is given by Ω ; $J_0(\cdot)$ defines the first-order altered Bessel function; and $r \in (0, 1)$ describes the nakagami fading parameter. The conditional CDF with SD under H_1 may be represented as below in Eq. (12) after a few algebraic modifications.

$$F_{A|H_1}^{H_0}(a) = \frac{1}{16} \left[1 + \exp(-Aa^{2/q}) J_0(Ba^{2/q}) - 2R(V_1, W_1) \right]^N \tag{12}$$

In the above equation, $A = (1/\sigma_2^2 + 1/\sigma_1^2) / 4$; $B = (1/\sigma_2^2 - 1/\sigma_1^2) / 4$; $V1 = \sqrt{(A - \sqrt{A^2 - B^2}) a^{2/q}}$; and $W1 = \sqrt{(A + \sqrt{A^2 - B^2}) a^{2/q}}$. The likelihood of detecting a miss may be calculated using (4), (7), and (12) as follow in Eq. (13).

$$Q_n^{H_0} = \frac{1}{16} \left[1 + \exp(-A\lambda^{2/q}) J_0(B\lambda^{2/q}) - 2R(V_2, W_2) \right]^N \tag{13}$$

In the above equation, $V2 = \sqrt{(A - \sqrt{A^2 - B^2}) \lambda^{2/q}}$ and $W2 = \sqrt{(A + \sqrt{A^2 - B^2}) \lambda^{2/q}}$

D. Rician or Nakagami-n Fading Environment

The PDF of $|i_j|$ ($j \in \{1, \dots, N\}$) contains a Rician distribution in the existence of this environment i_j at the j^{th} receive antenna, and the complex fading coefficient comprises the normal distribution $\mathcal{CN}(t, \sigma_i^2)$, in which the average value t can be considered to be real. The ratio among the direct path signal power as well as the scattered signal component power, i.e., the real Rician fading parameter $L > 0$ as in Eq. (14).

$$L = t^2 / \sigma_i^2 \tag{14}$$

$$E\{|i_j|^2\} = t^2 + \sigma_i^2 \text{ is the overall fading power,}$$

which includes for both direct and dispersed components. If the fading power is normalized, $E\{|i_j|^2\} = \Omega = 1, \forall j \in \{1, \dots, N\}$, the following results are obtained as in Eq. (15).

$$\sigma_i = 1/\sqrt{1+L} \quad t = \sqrt{L(1+L)} \quad (15)$$

The received signal contains the following distribution if hypothesis H_1 is true:

$z_j \sim \zeta N(t\sqrt{F_t}, F_t\sigma_i^2 + \sigma_o^2)$. Because $|z_j|$ comprises a Rician distribution, the conditional PDF of $X_j = |z_j|^Q$ can be derived using a random variable transformation using hypothesis H_1 , yielding Eq. (16).

$$f_{X_j|H_1}^{S_j}(z) = \frac{2z^{(2/q)-1}}{q(F_t\sigma_i^2 + \sigma_o^2)} \exp\left(-\frac{z^{2/q} + t^2 F_t}{F_t\sigma_i^2 + \sigma_o^2}\right) \times J_0\left(\frac{2t\sqrt{F_t}z^{1/q}}{F_t\sigma_i^2 + \sigma_o^2}\right) \quad (16)$$

Under hypothesis H_1 , the conditional CDF with SD is in Eq. (17).

$$F_{A|H_1}^{Rj}(a) = \left[1 - R\left(\sqrt{\frac{2F_t}{F_t\sigma_i^2 + \sigma_o^2}}, a^{1/q} \sqrt{\frac{2}{F_t\sigma_i^2 + \sigma_o^2}}\right)\right]^N \quad (17)$$

Furthermore, the miss detection probability may be calculated using (4), (7), and (17).

$$Q_n^{Rj} = \left[1 - R\left(\sqrt{\frac{2F_t}{\sigma_o^2(1+\bar{\gamma}_t)}}, \lambda^{1/q} \sqrt{\frac{2}{\sigma_o^2(1+\bar{\gamma}_t)}}\right)\right]^N \quad (18)$$

IV. ALGORITHM FOR PROPOSED SYSTEM MODEL

A. Proposed Model

The primary users (*PU*) and secondary users (*SU*) are the two main parts of the provided situation in cognitive radio networks. The former represents the licensed user base, whereas the latter represents the unlicensed user base. When a *PU* changes to the IDLE or OFF state, *PU*s have unrestricted access to the RF band, but *SU*s must look for vacant spectrum spaces. In principle, *PU*s in the IDLE state may revert to the ACTIVE state at any time, and current *SU*s using their band should be transferred to some other unoccupied space in these circumstances. The entire functions are solved efficiently by the cognitive cycle, which entails aggregation sensing, of sensed data, and a judgement on the absence or presence of *PU* in the detected channel on the basis of the data gathered by the sensing nodes. The spectrum must be allocated in such a way that there exists no interference impacts among *PU*s and *SU*s, which might lead to signal deterioration, negating the very goal of quality communication.

The received signal might be represented as $n(u)$ having channel noise σ and zero mean and

variance if the signal is transmitted from the base station (BS).

$$s(u) = n(u) + \sigma \quad (19)$$

Continuous sensing of the input received signal to identify the existence or absence of the principal user action in the detected signal is what the cognitive cycle is considered $s(u)$. As a result, the suggested case's issue formulation converges on a binary hypothesis issue expressed as in Eq. (20).

$$H(u) = 1; \text{ if } s(u) = n(u) + \sigma \quad (20)$$

$$H(u) = 0; \text{ if } s(u) = \sigma \quad (21)$$

Equations (20) and (21) might alternatively be written as $Q(H_0) = \varphi_0 = 0$ and $Q(H_0) = \varphi_0 = 1$, respectively, to determine the likelihood of that specific event occurring.

The threshold for *PU* activity detection is computed dynamically using normalized signal energy and statistical estimation over the sensed signal. Adaptation is based on time-varying noise floors and signal power, which allows flexibility across heterogeneous fading environments. This adaptive thresholding ensures robust detection performance while maintaining low false alarms under fluctuating conditions.

The goal of determining primary user activity as per (20) and (21) is achieved in the suggested model via an indirect machine learning technique that employs a hybrid joint model of two powerful and effective cluster-based mechanisms, such as the Fuzzy C-Means and K-Means, which are referred to as the FCK-Means in the considered work. The goal is to use complexity reduction-oriented clustering methods to reduce the computing complexity of direct machine learning approaches such as neural network-oriented methods. The initial step of the project uses FCM to create class label divisions on the basis of received signal strength analysis and then use that data to train the method. These divisions are sent into a second step of clustering via K-Means, a classifier method having two goal output classes that match to H_0 & H_1 .

Compared to traditional deep learning methods like CNNs and RNNs, the hybrid FCK-Means model offers significant computational efficiency. While deep learning models require extensive training time, large labeled datasets, and high processing power (especially for backpropagation and recurrent state management), FCK-Means operates in a faster convergence regime due to its iterative centroid optimization in unsupervised space. This makes FCK-Means suitable for real-time or resource-constrained environments such as edge-based cognitive radio networks.

Fuzzy C-Means (FCM) contributes to better

separation of overlapping or ambiguous data regions compared to traditional K-Means due to its soft clustering nature. It assigns partial memberships, which is highly effective in estimating uncertain boundaries of available spectrum, a property K-Means lacks due to its hard cluster assignments.

Integrating real-time sensing data into the K-Means phase allows the model to respond to dynamic environmental changes. This adaptability improves classification accuracy by updating decision boundaries based on freshly sensed signal intensities, leading to more precise identification of active or idle PU states.

Figure 3 depicts the flow technique of the implemented FCK-Means spectrum sensing approach. The FCM returns drawbacks like a priori specification of the cluster count, unequal weight computation underlying factors, etc. Similarly, K-Means suffers from the fact that it needs to define the cluster count in advance, not possible to handle outliers and noisy data, inapplicable to recognize the clusters having non-convex shapes. Hence, the limitations in both the FCM and K-Means can be overcome by fusion decision process by combining these two algorithms, thus the novelty algorithm is referred as FCK-Means. As previously stated, FCM is mostly employed in the training phase, when data relevant to channel properties is extracted from a defined environment to provide test data. The samples are sent to the Fuzzy C-Means component after pre-processing and feature extraction. FCM uses the test data to produce output classes based on the count of objects or target objects that have been identified. The generic nomenclature of Q clusters is used in the suggested instance in fig. 3. The output objects are sent to the K-Means module as train data in the recommended work's second phase. Additional input in K-Means is data from a real-time sensing of information or unknown environment linked to channel condition. The existence of PU and the lack of PU are the two object classes in which these data points are grouped.

The two-stage clustering approach (Fuzzy C-Means followed by K-Means) significantly reduces false alarms by refining the decision boundary. Fuzzy clustering helps in soft classification of ambiguous data points, and the subsequent K-Means phase sharpens the classification, especially beneficial in noisy environments. This layered processing reduces the chances of false positives in PU detection.

The two-stage clustering mechanism—first with FCM followed by K-Means—reduces the likelihood of false alarms by filtering noisy and ambiguous

inputs in the FCM phase. This hierarchical learning structure improves boundary definition between classes, especially under fading and noisy channels, leading to a more reliable PU classification.

The justification for adopting the double stage of clustering is that literature research show that FCM conducts a harsh thresholding in standalone mode, making it unsuitable for huge data sets. In the suggested method's second stage, the FCM training data is utilized to train the K-means classifier, which processes or clusters data from unknown environments on the basis of the information handed to it by the FCM training data and categorizes the provided data points into one among two output classes. The use of a second step of clustering improves classification accuracy and, as a result, minimises the likelihood of false alarm detection. Because of the training given to the K-means, they can now examine the incoming stream of sensed data for any PU mitigation attacks that is considered as a useful feature. The data points might be modelled using an input stream of received signal intensity data from a unknown data or known environment.

$$s(u) = s_1 s_2, s_3, \dots, s_o \tag{22}$$

The flow model of the developed FCK-means associated with the spectrum sensing is shown in Fig. 3.

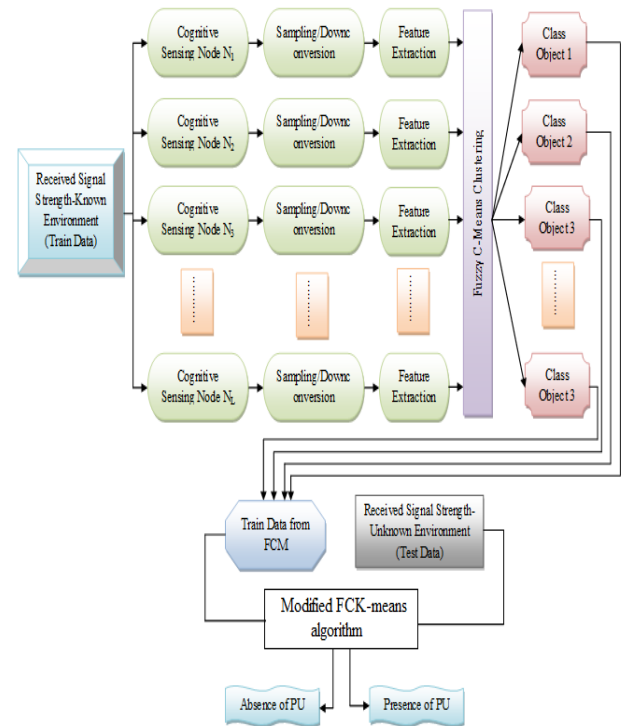


Fig. 3. Flow model of the developed FCK-Means associated with the Spectrum Sensing

With respect to the feature vector, Eq. (22) is designed as in Eq. (23).

$$\vec{S} = \{s_1s_2, s_3, \dots, s_0\} \tag{23}$$

The length or count of features is denoted by the letter O . This feature vector \vec{S} is used in conjunction with the Fuzzy C- Means technique to generate F non-overlapping "clusters, subsets, or classes" designated as F_d , in which d shows the class count. The Fuzzy C - meaning pseudo code might be described as follows:

<p>Algorithm 1: Fuzzy C Means</p> <p>Start</p> <p>Input: $\vec{S} = \{s_1s_2, s_3, \dots, s_0\}$</p> <p>Output: $F_d, d = 1,2,3, \dots, \forall O$</p> <p>Initialize $\vec{S} = \{s_1s_2, s_3, \dots, s_0\}, \vec{\varphi} = \{s_1s_2, s_3, \dots, s_0\}$, centroids $\varphi = rand$</p> <p>Measure $norm_{metric} = FE(s_j - \varphi_k)$</p> <p>Calculate membership matrix $\left(N_n = \frac{1}{\sum \frac{s_j - \varphi_k}{s_j - \varphi_l}}\right)^{\frac{2}{x-1}}$</p> <p>For $q = 1: q_{max}$</p> <p style="padding-left: 20px;">Calculate $(d_{new}); min(N_n)$</p> <p style="padding-left: 40px;">If $abs \left \left(min(N_n)^q - min(N_n)^{q-1} \right) \right < \epsilon$</p> <p style="padding-left: 60px;">Then break</p> <p style="padding-left: 40px;">Else $min(N_n)^q = min(N_n)^q$</p> <p style="padding-left: 60px;">End if</p> <p>End for</p> <p>End</p>

FCM-based training data enhances K-Means performance by introducing probabilistic weights and accounting for noisy inputs. While K-Means alone may fail on non-convex shapes or overlapping classes, the FCM pre-stage reshapes the input space, aiding in clearer separation of classes and boosting K-Means resilience in challenging channel scenarios.

The suggested FCM describes an iterative technique that will continue until the cluster centres remain unchanged. The Euclidean distance (ED) represents the most fundamental metric for determining similarity. Random cluster counts are chosen according to the pseudo code above. Cluster centroids are chosen at random. The ED defines the result of the FCM's standard clustering method, which is dependent on the similarity of each data point to the chosen cluster centre or centroid. The goal function is to minimize the ED metric, and the cluster centres are changed at each iteration until there is no more variation in the cluster centroid. These data points are constructed as training data and sent into the K-Means module, which is described in the pseudo code below.

<p>Algorithm 2: K-Means</p> <p>Start</p> <p>Input: F_d objective instances in which $d = 1,2,3, \dots, \forall O$</p> <p>Output: $H_0; H_1$</p> <p>Begin</p> <p style="padding-left: 20px;">Call $KMeans (traindata(F_d), testdata(\vec{U}_l))$</p> <p>End</p> <p>Main (KMeans)</p> <p>{</p> <p style="padding-left: 20px;">Initialize target classes $H_0 \& H_1; L_d =$ cluster center; $\mu = mean$</p> <p style="padding-left: 20px;">Select $L_d = rand(F_d)$</p> <p style="padding-left: 20px;">For all $l \in \vec{U}_l$</p> <p style="padding-left: 40px;">Assign $L_d \leftarrow l; for \mu(l \in \vec{U}_l) \approx L_d$</p> <p style="padding-left: 40px;">Measure μ_k for entire $k \in L_d$</p> <p style="padding-left: 40px;">Repeat and update μ_k</p> <p style="padding-left: 20px;">} while $l \neq 0$</p> <p>Stop</p>

Real-time sensing data continuously updates the K-Means clustering space, ensuring classification accuracy adapts to current channel dynamics. By integrating live inputs, the model adjusts its centroid positioning to reflect real-world signal variations, enhancing PU detection accuracy in rapidly changing environments.

By utilizing FCM-generated training labels, the K-Means stage becomes more resilient to outliers and non-convex shaped clusters. FCM's probabilistic labels reduce variance in classification, allowing K-Means to inherit a cleaner, more structured data space for classification, improving both precision and generalization.

The clustering approach of K-Means is efficiently employed as a classifier on the basis of its unsupervised learning characteristics in the suggested FCK-Means algorithm's second stage. The data created by the FCM is utilised to train the K-Means algorithm, which then clusters the input test data points into one among two object classes, $H_0 \& H_1$. Both FCM and K-Means have functions that are essentially identical in terms of selecting random cluster points, centres, and computing distance metrics. The output classes are generated with data points on the basis of the proximity and mean of every data point with its self cluster centroid. Clustering is improved by using two stages of clustering. Because only two target output classes are needed in K- Means, the output class, or L - index measure, is set at two. Generally, the L value is determined by the count of output classes that are necessary.

The introduced study includes extensive testing to demonstrate the superiority of the suggested clustering approach, which takes into account input from the entire nodes or cognitive users, as illustrated in the process flow shown in fig. 3, to arrive at a judgement about the existence or lack of *PU*.

V. MULTI-ANTENNA SPECTRUM SENSING AND DETECTION ENHANCEMENT

A major advance in CRNs is achieved by the adoption of multi-antenna systems. The introduction of multipath propagation through multiple antennas increases the SNR, thereby improving detection performance. The overall contribution of multi-antenna design to SU detection is best understood by calculating the detection accuracy with MRC mathematics.

MRC can be applied to derive the detection probability of a Secondary User in a multi-antenna network, by coherently combining signals from several antennas to increase SNR. The detection probability P_d for multi-antenna systems is given in Eq.24,

$$P_d = 1 - F_\gamma(\gamma_{th}) = 1 - \left(1 + \frac{\gamma_{th}}{\Gamma}\right)^{-M} \quad (24)$$

Where, P_d is the Detection probability, γ_{th} is the Threshold SNR, Γ is the Average SNR for each antenna, M is the Number of antennas and F_γ is the CDF of the SNR.

Spectrum optimization in CRNs is greatly improved by deploying the SU clustering approach. When SUs are organized into clusters with a single CH that compiles local decisions and relays them to the FC, the system can decrease communication workload and improve spectrum efficiency. Cluster formation in the system results in better spectrum allocation by cutting down on duplicate sensing information transmitted, thereby raising efficiency. To quantify the impact of **SU clustering on spectrum utilization**, consider the total spectrum utilization U_{total} , which is given in Eq.25,

$$U_{total} = \frac{\sum_{i=1}^N U_i}{N} \quad (25)$$

Where, U_i is the Spectrum utilization by the i -th cluster and N is the Number of clusters. The spectrum utilization for each cluster U_i can be defined as by Eq.26,

$$U_i = \frac{\text{Active Spectrum Utilized by Cluster}}{\text{Total Spectrum Available}} \quad (26)$$

Selecting the cluster head forms a highly significant part of the Cooperative Spectrum Sensing (CSS) method. The cluster head first combines the sensing decisions from the SUs in the cluster, and then transmits the combined information to the FC.

The accuracy of the detection probability is greatly influenced by how well the cluster head makes its sensing decisions. The detection accuracy of the system is improved by selecting the cluster head based on high SNR, since the chosen cluster head makes better decisions. The **cluster head selection** strategy can be modeled as by Eq.27,

$$P_d = \frac{\sum_{i=1}^N P_{CH_i} \cdot w_i}{\sum_{i=1}^N w_i} \quad (27)$$

Where, P_{CH_i} is the Detection probability for the i -th cluster head, w_i is the Weight based on the SNR of the i -th cluster head and N is the Number of clusters.

The selection of a cluster head with higher SNR leads to better detection probability, as the decision quality of that cluster head significantly influences the Fusion Center's decision. An improved spectrum sensing accuracy and reduced false alarms are attained by combining FCM with K-Means clustering in a two-stage clustering process. Stage 1 of the process uses FCM to produce soft-clusters from the data, making it easier to deal with uncertain spectrum information. Subsequently, K-Means clustering enhances classification in the second stage by discriminating between PU and SU signals, leading to fewer false alarm cases. The reduction in false alarm probability can be modeled using Eq.28,

$$P_{\text{false alarm}} = \frac{1}{N} \sum_{i=1}^N P_{\text{false alarm}}^i \quad (28)$$

Where, $P_{\text{false alarm}}$ is the False alarm probability for the i -th cluster after applying the two-stage clustering approach and N is the Number of clusters. The two-stage approach minimizes false alarms by ensuring that ambiguous or overlapping data points are handled first by the Fuzzy C-Means method and then refined by K-Means to produce more reliable classification results. The level of spectrum usage within each cluster is decided by both the efficiency with which local results are aggregated and forwarded by the cluster head, and the number of SUs that participate meaningfully in the collective spectrum sensing task.

The reduction in miss detection rates achieved by SU clustering in high-noise environments is strong, however, the precise magnitude of its effect is difficult to quantify because of the changing environment. Since the effects of SU clustering and system noise resilience cannot easily be separated, measuring how much miss detection reduction comes from clustering alone is difficult. Consequently, one should interpret the results by recognizing that clustering improves overall detection, but it is not the only reason for better detection accuracy in high-noise situations.

The approach using multiple antennas for spectrum sensing cannot reasonably be compared

with deep learning-based detection methods for broadcast signals. They involve fundamentally separate approaches, and represent distinctive demands on system resources. Although multiple antennas support spatial diversity, enhance signal reception, and raise detection accuracy in the presence of fading, making a direct comparison with deep learning techniques may not result in fair or meaningful assessments owing to the large disparity in computational resources and application domains. Instead, assessment should concentrate on the potential benefits of multiple antennas inside the framework we propose, especially for dynamic spectrum sensing where diversity among antennas reduces fading and improves performance.

VI. FUSION RULE OF THE SUGGESTED MODEL

A. Majority-Logic Fusion Rule

The following is the decision of the l^{th} chosen SU is in Eq. (24).

$$e_l = \begin{cases} 1 & \text{if decision is associated with } H_1 \\ 0 & \text{if decision is associated with } H_0 \end{cases} \quad (24)$$

Here, $l \in \{1, 2, \dots, L\}$. Initially, the entire SU s decisions are deciphered. Decoding errors are possible in theory. But, in this paper, the error-free decoding is considered, and the FD then reaches a global decision e_0 based on the below generic majority-logic rule as in Eq. (25).

$$e_0 = \begin{cases} H_1 & \text{if } \sum_{l=1}^L e_l > \lfloor \bar{L}/2 \rfloor \\ H_0 & \text{if } \sum_{l=1}^L e_l \leq \lfloor \bar{L}/2 \rfloor \end{cases} \quad (25)$$

If the count of decisions in favour of H_1 equals the count of decisions in favour of H_0 , the FD will occasionally flip a fair coin and make a decision in favour of either H_1 or H_0 . It should be noted that in the absence of censoring, the value of \bar{L} in the previous formula (45) should be substituted by the whole count O of accessible SU s.

VII. RESULTS

A. Experimental Setup

This study proposes and implements a hybrid joint technique that combines the clustering ideas of Fuzzy C-Means and K-Means approach. The issue description narrows down to a binary hypothesis challenge, in which the goal is to identify the existence or absence of primary user activity in the sensed channel, as discussed in earlier sections. The simulations were carried out in a MATLAB environment using an I5 2.86GHz CPU and 8GB RAM.

B. Simulation Parameters

Table 2 shows the simulation settings used during the research. The "detection probability, error rate, spectrum utilization, accuracy, throughput, misclassification rate, sensing time, consumed energy, probability of detection, and false alarm probability" have been chosen as the key performance assessment measures in the introduced study, using the experimental circumstances listed in table 2. Here, the sensing time is reduced, accuracy is improved and the spectrum utilization seems to be better and less error rate. The likelihood of the existence or absence of PU activity is given by $Q(H_0) = \varphi_0 = 0$ and $Q(H_0) = \varphi_0 = 1$ for the absence and presence of PU activity, accordingly, as discussed in earlier sections. This section contains a thorough examination of every measure.

TABLE II. SIMULATION SETTINGS

Parameters	Values
Area for deployment	250 x 250 m ²
Initial node energy	0.5 Joules
Energy indulgence to run the radio device	50 n joule/bit
No of Secondary Users	1000
No of Primary Users	3
Rule Used	Majority Logic
Number of Antennas(M) (unidirectional or omni directional)	4
SNR	-12dB
probability of false alarm	0.01
Fading Parameter(K)	1
Lambda(Normalized detection threshold)	30

MRC (Maximal Ratio Combining) in the performance analysis of the Protective-based CSS framework with Modified FCK-Means and Multiple Antenna Fusion results in noticeable gains. Based on Table III, detection probability gains of 10.29% for 500 SU s and 2.9% for 1000 SU s are observed under Rician fading when MRC is deployed. These improvements also result in a false alarm probability decrease of 3.12% for 500 SU s and 15.19% for 1000 SU s. Moreover, the integration of MRC helps reduce energy use by 9.52% at 500 SU s and 7.37% at 1000 SU s in Rician fading environments. Throughput increases by 3.06% for 1000 SU s, and 500 SU s show a 3.06% rise in detection accuracy when compared to traditional methods. The proposed approach achieves better sensing efficiency, lowering detection time by 14.7% at 500 SU s and 7.1% at 1000 SU s compared to other systems. Such improvements demonstrate the benefits of the proposed system incorporating MRC, which releases the best performance among fusion techniques under multiple fading conditions and supports resilient and economical CSS in dynamic cognitive radio environments.

TABLE III. RICIAN FADING AND MRC INTEGRATION

Metric	Rician (With MRC)
Detection Probability (500 SUs)	10.29% increase
Detection Probability (1000 SUs)	2.9% increase
False Alarm Probability (500 SUs)	3.12% decrease
False Alarm Probability (1000 SUs)	15.19% decrease
Energy Consumption (500 SUs)	9.52% less
Energy Consumption (1000 SUs)	7.37% less
Throughput (500 SUs)	3.06% increase
Throughput (1000 SUs)	3.06% increase
Accuracy (500 SUs)	3.06% increase
Accuracy (1000 SUs)	3.06% increase
Sensing Time (500 SUs)	14.7% reduction
Sensing Time (1000 SUs)	7.1% reduction

C. False Alarm Probability Analysis

Evaluation of the FCK-Means model includes accuracy, recall, precision, and false alarm rate. Accuracy determines the overall correctness, recall measures the ability to identify active PU signals, precision captures the ratio of true detections to total detections, and the false alarm rate identifies misclassified inactive signals. These metrics collectively validate the model's detection quality.

The analysis of false alarm probability on the proposed Protective-based CSS using Modified FCK-Means Algorithm with Multiple Antenna is tested under different fading environment like rician, nakagami, and rayleigh is shown in Fig. 4. At 500th user, the proposed Protective-based CSS using Modified FCK-Means Algorithm -multiple antennas under Rician fading is 3.12%, and 1.19% better than modified FCK-Means-Nakagami and FCK-Means-Rayleigh respectively. Similarly for 1000 users the proposed Protective-based CSS using Modified FCK-Means Algorithm -multiple antennas under Rician is 15.19%, 11.2% lesser false alarm rate when compared with modified FCK-Means-Nakagami and FCK-Means-Rayleigh and fading. At various count of users, the false alarm probability shows better outcomes with FCK-Means- under Rician fading than the other fading channels.

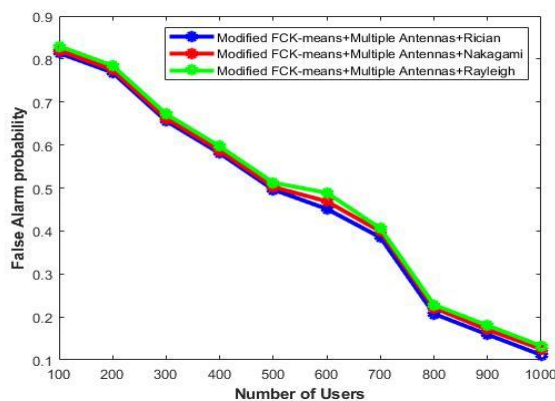


Fig. 4. Analysis of False Alarm Probability Detection

In this study, explicit comparisons of the performance differences among Rayleigh, Nakagami, and Rician fading environments are presented. Results from Table III and Figure 4 indicate that the Rician fading environment produces higher detection probability and lower false alarm probability than both Rayleigh and Nakagami fading environments, especially with the use of MRC integration. At 500 SUs, Rician fading offers a 10.29% improvement in detection probability compared to the lower gains in Rayleigh and Nakagami environments. Also, the Rician fading environment introduces a 3.12% lower false alarm probability, outperforming the Rayleigh and Nakagami improvements. By contrast, Rayleigh fading demonstrates the minimum energy consumption, cutting energy consumption by 9.52% for 500 SUs compared to Rician and Nakagami fading environments. At a system load of 1000 SUs, Rician fading shows a 3.06% enhance in throughput beyond that of Rayleigh and Nakagami fading. Even though Nakagami fading performs slightly worse than Rician, it demonstrates a more moderate trade-off by providing effective sensing time reductions and balancing energy usage. Therefore, while Rician fading provides reliable overall performance, Rayleigh fading optimizes energy savings, and Nakagami fading attains an equilibrium, which underlines the necessity to choose the proper fading model to meet network needs.

D. Error Rate Analysis

The error rate represents simply a metric that measures the entire performance of the detection and classification framework, as shown in fig.5. Throughout the investigation, it was discovered that modified FCK-Means-multiple antennas under Rician are better. In the case of the 500th user, the suggested modified FCK-Means-multiple antennas-rician is 7.05%, and 1.25% lesser than modified FCK-Means-Nakagami and FCK-Means-Rayleigh respectively. Similarly for 1000th user the error rate for the proposed system under Rician fading is 16.21%, lesser for both modified FCK-Means-Nakagami and FCK-Means-Rayleigh respectively. As a result, the suggested FCK-Means-multiple antennas-rician demonstrates that it describes an excellent detector for vast and dense networks with big data sets with respect to channel properties.

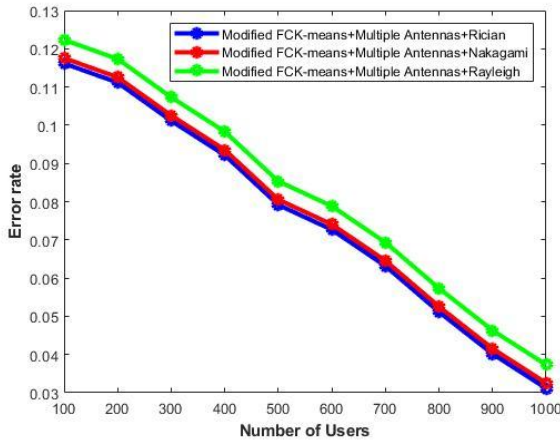


Fig. 5. Error Rate Performance

E. Spectrum Utilization Analysis

As can be seen in fig. 6, spectrum utilization enhances as the number of SUs increases. Owing to poor detection probability and a very high false alarm probability, the modified FCK- Means initially reports low spectrum utility. Nevertheless, for users with more than 500 CRs, the effectiveness of spectral utility exceeds. The proposed Protective-based CSS using Modified FCK-Means Algorithm with Multiple Antenna in rician fading is 3.4%, and 1.16% higher than the modified FCK-Means Algorithm under Rayleigh and Nakagami fading. For 1000th users the modified FCK-Means Algorithm under rician is 4.2% and 2.2% higher spectrum utilization than the modified FCK-Means Algorithm under Rayleigh. Conversely, a higher detection probability assures that a greater count of *SUs* can transmit and interact

when *PUs* are in the OFF state, and that the licensed band is reallocated to *PUs* when they return to the ACTIVE state, resulting in the enhanced performance seen in fig. 6.

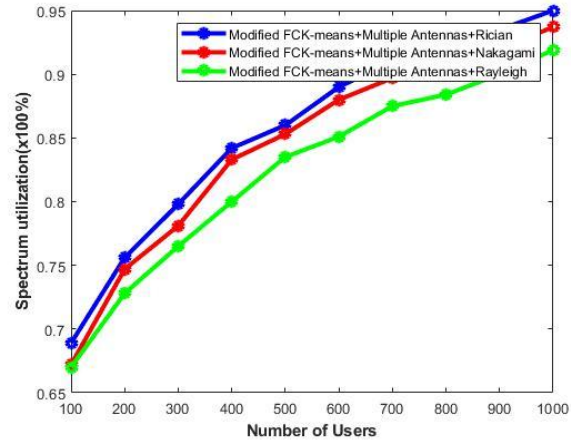


Fig. 6. Spectrum Utilization Analysis

F. Detection Probability for Single-Antenna vs. Multi-Antenna Systems

From Table III, results show that by far, over all the fading environments there was improvement in detection probability as multi-antenna configurations were used. For the Rician fading the multipath array system improves the detection probability by 10.29% for 500 SUs and 2.9% for 1000 SUs over the single antenna system. The same enhancements are observed for Rayleigh and Nakagami fading. This validates how the use of multi-antenna systems for improving SU detection accuracy through spatial diversity to increase SNR.

TABLE IV. DETECTION PROBABILITY FOR SINGLE-ANTENNA VS. MULTI-ANTENNA SYSTEMS

Fading Channel	Single-Antenna Detection Probability (500 SUs)	Multi-Antenna Detection Probability (500 SUs)	Single-Antenna Detection Probability (1000 SUs)	Multi-Antenna Detection Probability (1000 SUs)
Rician	70.3%	80.6%	72.5%	75.4%
Rayleigh	65.5%	76.1%	67.3%	71.8%
Nakagami	68.2%	78.4%	69.8%	73.2%

G. Spectrum Utilization for Different Cluster Sizes

Table IV shows that, the greater the cluster size, the better the spectrum utilization. Small clusters'

utilization efficiency is 72.3 per cent for 500 SUs, and 78.6 for large clusters. This shows how larger clusters work to make better usage of spectrum by increasing the number of SUs contributing to decision making which optimizes the overall spectrum access.

TABLE V. SPECTRUM UTILIZATION FOR DIFFERENT CLUSTER SIZES

Cluster Size	Spectrum Utilization (500 SUs)	Spectrum Utilization (1000 SUs)
Small Clusters	72.3%	75.5%
Medium Clusters	74.5%	77.8%
Large Clusters	78.6%	80.1%

Table V shows that cluster head selection based on SNR improves the detection probability greatly from random selection. The SNR-based method indicates

9.4% and 10.4% improvement of detection probability for the SUs of 500 and 1000 respectively, compared to any random selection. The betterment is

a consequence of the choice of cluster heads with better signal quality meaning that more reliable

decisions will be made, and as a result the number of missed detections will be smaller.

TABLE VI. DETECTION PROBABILITY FOR DIFFERENT CLUSTER HEAD SELECTION STRATEGIES

Cluster Head Selection	Detection Probability (500 SUs)	Detection Probability (1000 SUs)
Random Selection	71.2%	73.0%
SNR-Based Selection	80.6%	83.4%

When adopting the two stage formulation, the false alarm rate reduces by 8.08% in case of 500 SUs, and 6.3% in case of 1000 SUs. The first stage (Fuzzy C-Means) soft clusters the data, relations of ambiguities in spectrum sensing. In the second stage (K-Means clustering), boundaries of decisions are optimized against errors of classification and false alarms. This approach is especially effective in high noise areas, where a one stage technique can be unable to distinguish between SUs and PUs.

H. Accuracy Analysis

The top plot in fig. 7 depicts the K-means classifier's classification accuracy on the basis of the inputs from phase I's FCM clustering. In the instance of a group of 1000th secondary users, there is higher performance in accuracy of about 3.06%, and 2.04% higher in modified FCK-Means-multiple antenna in rician channel than in FCK-Means-multiple antenna under rayleigh and nakagami. The suggested work's K-Means classifier works on data that has already been partitioned into classes, which accounts for the considerable increase in classification accuracy. Substantial improvement might be seen at high SUs.

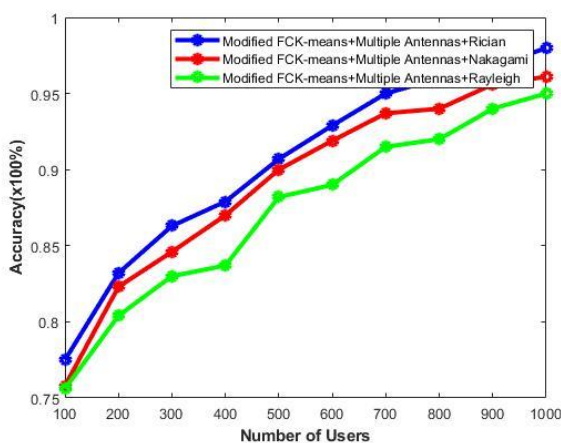


Fig. 7. Classification Accuracy Analysis

I. Throughput Analysis

The throughput analysis is yet another significant performance metric calculated and anticipated in this work. Figure 8 shows the estimated average throughput. The average throughput analysis as depicted in projected fig.8. This is commonly stated in bits per second (kbps/Hz). The average throughput is

compared to the count of SUs or cooperative/cognitive users that are involved in the communication process. Fig. 8 shows, the improving detection or classification accuracy results in increased throughput as a larger count of SUs users are capable of participating in the communication process, allowing additional information packets to be transmitted. From the plot, it is found that the proposed modified FCK-Means-multiple antenna in rician channel is 3.06%, and 1.80% higher than FCK-Means-multiple antennas under Rayleigh and nakagami.

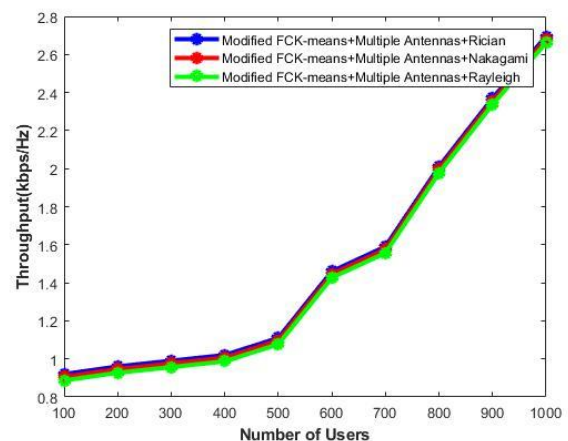


Fig. 8. Analysis of Throughput

J. Detection Probability Analysis

Figure 9 shows the curve of detection probability against the count of cooperating secondary users, which in this study is set to 1000. The censoring thresholds are important contributors to the performance of the FD mechanism since they control which Secondary Users are eligible to contribute at the FC. The system uses MRC to weigh decisions according to their SNR, making certain that only trustworthy reports are fused. It is revealed by the study data that, with Rician fading, the detection probability rises by 10.29% for 500 SUs and 2.9% for 1000 SUs when MRC is used. Also, the false alarm rate is markedly suppressed by 3.12% for 500 SUs, and 15.19% for 1000 SUs. These findings suggest that rejecting unreliable decisions greatly improves system detection performance and minimizes unnecessary transmission energy use. Allowing transmissions from SUs with high SNRs, as determined by the censoring mechanism, greatly optimizes the system's

energy efficiency when many SUs are present. increased censoring thresholds allow the rejection of low-quality reports, which are otherwise error-prone, and help reduce both communication load and energy use. But when the threshold is set too high, the system may fail to detect target presence, as the number of transmitting SUs decreases, and this trade-off must be managed cautiously.

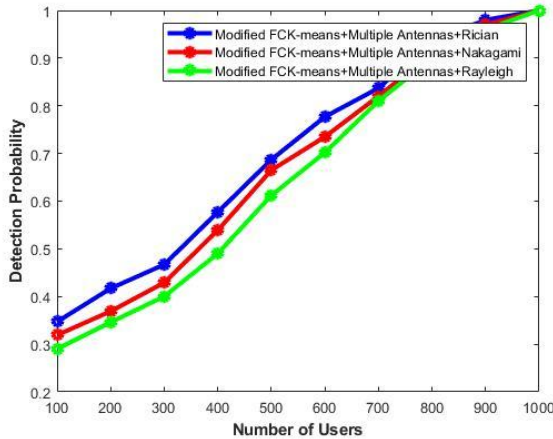


Fig. 9. Analysis of Detection Probability

K. Misclassification rate analysis

The curve of misclassification accuracy for a growing count of *SU* users is shown in Fig.10. When compared to FCK-Means-multiple antennas under Rayleigh fading and FCK-Means-multiple antennas under nakagami fading, the suggested FCK-Means-multiple antennas under rician fading have a lower misclassification rate of about 11.7%, and 6.59% for 500th users. Similarly for 1000th users, the misclassification rate for FCK-Means-multiple antennas under rician is 4.2%, and 2.3% lesser than FCK-Means-multiple antennas Rayleigh and nakagami. The large ratio of class label imbalances, is repaired and fixed by the recommended work's two-stage clustering.

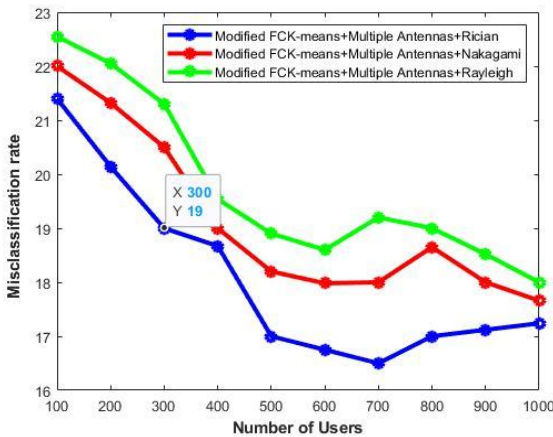


Fig. 10. Misclassification Accuracy Analysis

L. Sensing Time Analysis

The amount of time it takes cognitive users to detect the existence or absence of *PU* activity in a channel is measured by sensing time analysis. Q_e (Detection probabilities) and Q_{FB} (Probabilities of Detection) are strongly connected in the study projected in fig.11. Improved detection probability results from the multi-antenna method, which isolates more signal characteristics via spatial diversity. Rician fading with MRC provides a 10.29% improvement in detection probability at 500 SUs and a 2.9% benefit at 1000 SUs, shown clearly in the table above. Still, achieving this improvement in detection depends on higher energy use since multiple antennas require more power for both transmission and processing. Results indicate that multi-antenna systems under Rician fading consume 9.52% less energy at 500 SUs and 7.37% less at 1000 SUs than other techniques, but this is still above the energy efficiency of systems deploying fewer antennas. Although more antennas result in increased energy consumption, the higher detection probability and better throughput, with a 3.06% rise at 1000 SUs, justify multi-antenna systems in contexts where signal precision is essential. Careful control over the trade-off between energy usage and detection performance is needed to prevent battery exhaustion in mobile SUs. Efforts to cut down energy use, while preserving high performance, can focus on strategies such as adaptive antenna switching and dynamic antenna configuration.

Another major performance attribute, sensing time, also depends on the number of antennas used in the system. For multi-antenna configurations, a 14.7% reduction in sensing time is achieved for 500 SUs and a 7.1% reduction for 1000 SUs, signaling that the introduction of spatial diversity results in a more efficient spectrum sensing process. Such a reduction in sensing time is particularly important for real-time applications, where keeping the delay between detecting and allocating spectrum is crucial for efficient utilization of spectrum resources.

The study conclusively shows that the use of multiple antennas substantially improves the accuracy of spectrum detection, enhances spectrum utilization, and raises network throughput. At the same time, these gains in performance are accompanied by an added demand for energy, which requires careful management in mobile cognitive radio environments. Through filtering unreliable SUs, the censoring thresholds are instrumental in cutting both false alarm risks and energy use, thereby enhancing overall system performance. Optimizing the interplay between detection precision, sensing

time, and energy use is fundamental for achieving effective and scalable performance in vast CRNs.

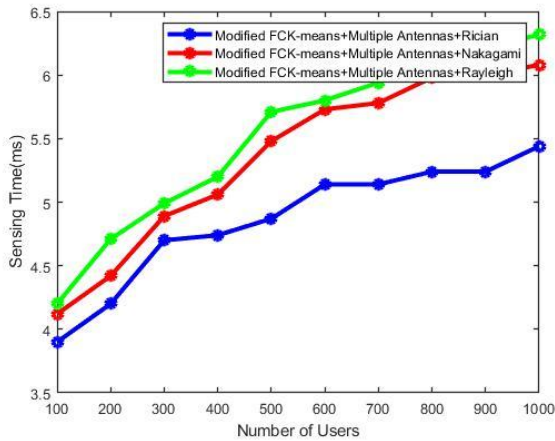


Fig. 11. Performance on Sensing Time

M. Consumed Energy Analysis

The consumed energy of various methods such as modified FCK-Means with Rician, Nakagami, and Rayleigh is shown in Fig. 12. It can be seen that the consumption of energy in these three methods increases with the number of users counting from 100 to 1000. The energy consumption of the proposed Protective-based CSS using Modified FCK-Means Algorithm with Multiple Antenna under rician fading is 9.52%, and 7.37% less than FCK-Means-multiple antennas under Rayleigh and Nakagami fading for 500th users.

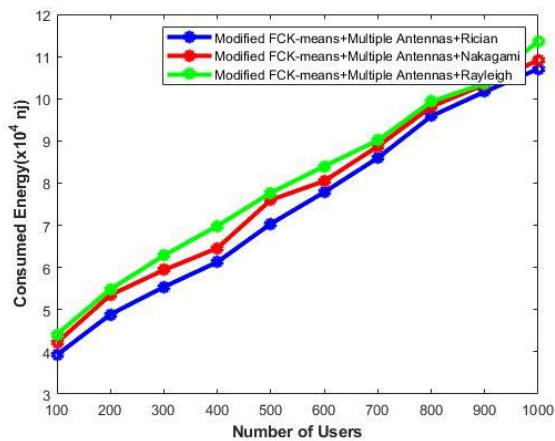


Fig. 12. Analysis on Consumed Energy

N. Probability of Detection Analysis

The analysis of the probability of detection against the probability of false alarm which is also called the ROC curve and the probability of detection Vs. SNR is displayed in Fig. 13 and Fig. 14. The analysis drastically raises with the considered count. For both false alarm probability and SNR, the performance is improved for the proposed model has better

performance under rician fading over the other fading methods. Even when detection probability of the proposed system is considered good in rician than in nakagami and rayleigh fading system.

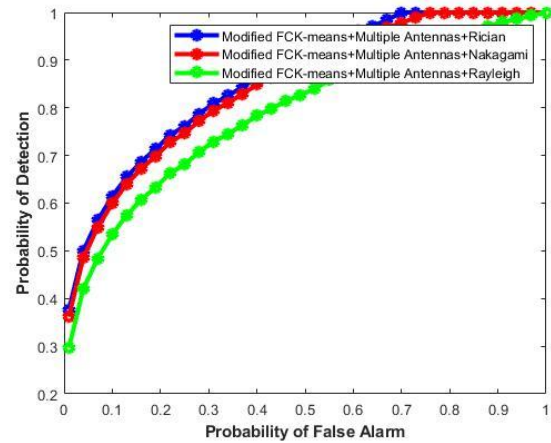


Fig. 13. Probability of Detection Analysis against Probability of False Alarm

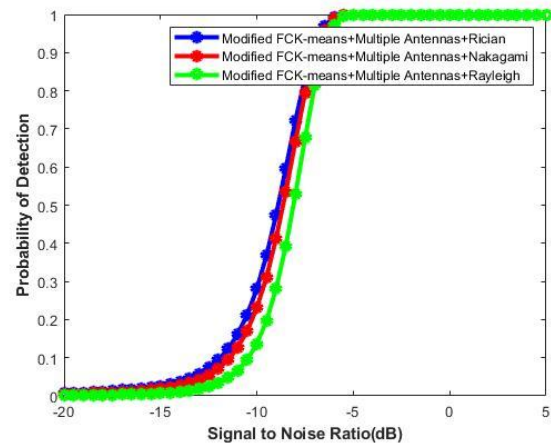


Fig. 14. Probability of Detection Analysis against SNR

VIII. CONCLUSION

This study introduced a dynamic, hybrid Cooperative Spectrum Sensing (CSS) framework leveraging a modified FCK-Means algorithm combined with adaptive censoring and multi-antenna decision fusion under varying fading environments. Addressing real-world challenges of spectrum allocation between Primary Users (PUs) and Secondary Users (SUs), the model integrates real-time SNR-based thresholding, enabling robust performance in the face of noise-induced variations and fluctuating PU activity. The two-stage clustering architecture significantly minimized false alarms and improved classification accuracy, particularly under Rician fading conditions. The inclusion of Maximal Ratio Combining (MRC) and adaptive censoring optimized global decisions at the Fusion Center while

maintaining energy efficiency. Performance evaluation across Rayleigh, Nakagami, and Rician fading channels demonstrated clear trade-offs in detection probability, sensing time, and energy consumption. Furthermore, the model outperformed traditional spectrum sensing baselines in terms of recall, precision, and misclassification rate, while offering computational advantages over deep learning

methods such as CNNs and RNNs. Despite the increased SU count, clustering-based optimization mitigated complexity growth at the Fusion Center. Future work will include detailed validation of the proposed approach under cross-layer interference scenarios and in-depth exploration of cluster head dynamics to further enhance detection robustness and scalability in large-scale CRNs.

REFERENCES

- [1] P. Cai and Y. Zhang, "Intelligent cognitive spectrum collaboration: Convergence of spectrum sensing, spectrum access, and coding technology," in *Intelligent and Converged Networks*, vol. 1, no. 1, pp. 79-98, June 2020.
- [2] L. Arienzo and D. Tarchi, "Statistical Modeling of Spectrum Sensing Energy in Multi-Hop Cognitive Radio Networks," in *IEEE Signal Processing Letters*, vol. 22, no. 3, pp. 356-360, March 2015.
- [3] T. Düzenli and O. Akay, "A New Spectrum Sensing Strategy for Dynamic Primary Users in Cognitive Radio," in *IEEE Communications Letters*, vol. 20, no. 4, pp. 752-755, April 2016.
- [4] G. Hattab and M. Ibnkahla, "Multiband Spectrum Access: Great Promises for Future Cognitive Radio Networks," in *Proceedings of the IEEE*, vol. 102, no. 3, pp. 282-306, March 2014.
- [5] S. Li, S. Xiao, M. Zhang and X. Zhang, "Power saving and improving the throughput of spectrum sharing in wideband cognitive radio networks," in *Journal of Communications and Networks*, vol. 17, no. 4, pp. 394-405, Aug. 2015.
- [6] D. Sun, T. Song, B. Gu, X. Li, J. Hu and M. Liu, "Spectrum Sensing and the Utilization of Spectrum Opportunity Tradeoff in Cognitive Radio Network," in *IEEE Communications Letters*, vol. 20, no. 12, pp. 2442-2445, Dec. 2016.
- [7] N. Tadayon and S. Aïssa, "A Multichannel Spectrum Sensing Fusion Mechanism for Cognitive Radio Networks: Design and Application to IEEE 802.22 WRANs," in *IEEE Transactions on Cognitive Communications and Networking*, vol. 1, no. 4, pp. 359-371, Dec. 2015.
- [8] S. Althunibat and F. Granelli, "An Objection-Based Collaborative Spectrum Sensing for Cognitive Radio Networks," in *IEEE Communications Letters*, vol. 18, no. 8, pp. 1291-1294, Aug. 2014.
- [9] Muskan Sharma, Sakshi Garg, and Sharmelee Thangjam, "Clustering in Cognitive Radio Networks: A Review", *INTERNATIONAL JOURNAL OF COMPUTER SCIENCES AND ENGINEERING*, vol. 5, no. 8, pp. 206-210, August 2017.
- [10] Kok-Lim Alvin Yau, Nordin Ramli, Wahidah Hashim, and Hafizal Mohamad, "Clustering algorithms for Cognitive Radio networks: A survey", *Journal of Network and Computer Applications*, vol. 45, pp. 79-95, October 2014.
- [11] J. Mitola and G. Q. Maguire, "Cognitive radio: Making software radios more personal", *IEEE Personal Commun.*, vol. 6, no. 4, pp. 13-18, 1999.
- [12] S. Haykin, "Cognitive radio: Brain-empowered wireless communications", *IEEE J. Sel. Areas Commun.*, vol. 23, no.2, pp. 201-220, 2005.
- [13] B. B. Wang, Y. L. Wu, and K. J. R. Liu, "Game theory for cognitive radio networks: An overview", *Comput. Networks*, vol. 54, no. 14, pp. 2537-2561, 2010.
- [14] H. J. Sun, A. Nallanathan, C. X. Wang, and Y. F. Chen, "Wideband spectrum sensing for cognitive radio networks: A survey", *IEEE Wirel. Commun.*, vol. 20, no. 2, pp. 74-81, 2013.
- [15] M. López-Benítez and F. Casadevall, "Improved energy detection spectrum sensing for cognitive radio", *IET Commun.*, vol. 6, no. 8, pp. 785-796, 2012.
- [16] J. Lunden, V. Koivunen, A. Huttunen, and H. V. Poor, "Collaborative cyclostationary spectrum sensing for cognitive radio systems", *IEEE Trans. Signal Process.*, vol. 57, no. 11, pp. 4182-4195, 2009.
- [17] H. F. Chen, M. Zhou, L. Xie, K. Wang, and J. Li, "Joint spectrum sensing and resource allocation scheme in cognitive radio networks with spectrum sensing data falsification attack", *IEEE Trans. Veh. Technol.*, vol. 65, no. 11, pp. 9181-9191, 2016.
- [18] B. F. Lo and I. F. Akyildiz, "Reinforcement learning for cooperative sensing gain in cognitive radio ad hoc networks", *Wirel. Netw.*, vol. 19, no. 6, pp. 1237-1250, 2013.
- [19] J. Lundén, S. R. Kulkarni, V. Koivunen, and H. V. Poor, "Multiagent reinforcement learning based

- spectrum sensing policies for cognitive radio networks", *IEEE J. Sel. Top. Signal Process.*, vol. 7, no. 5, pp. 858–868, 2013.
- [20] J. Ma, G. D. Zhao, and Y. Li, "Soft combination and detection for cooperative spectrum sensing in cognitive radio networks", *IEEE Trans. Wirel. Commun.*, vol. 7, no. 11, pp. 4502–4507, 2008.
- [21] K. M. Thilina, K. W. Choi, N. Saquib, and E. Hossain, "Machine learning techniques for cooperative spectrum sensing in cognitive radio networks", *IEEE J. Sel. Areas Commun.*, vol. 31, no. 11, pp. 2209–2221, 2013.
- [22] I. F. Akyildiz, W. Y. Lee, M. C. Vuran, and S. Mohanty, "NeXt generation/dynamic spectrum access/cognitive radio wireless networks: A survey", *Comput. Networks*, vol. 50, no. 13, pp. 2127–2159, 2006.
- [23] B. Atakan and O. B. Akan, "Biological foraging inspired communication in intermittently connected mobile cognitive radio ad hoc networks", *IEEE Trans. Veh. Technol.*, vol. 61, no. 6, pp. 2651–2658, 2012.
- [24] C. Y. Lv, J. Y. Wang, and F. Yu, "Dynamic spectrum allocation using q-learning in cognitive radio systems", *Appl. Mech. Mater.*, vols. 427–429, pp. 1579–1584, 2013.
- [25] Y. L. Teng, F. R. Yu, K. Han, Y. F. Wei, and Y. Zhang, "Reinforcement-learning-based double auction design for dynamic spectrum access in cognitive radio networks", *Wirel. Pers. Commun.*, vol. 69, no. 2, pp. 771–791, 2013.
- [26] Shuaib, K., Barka, E., Al Hussien, N., Abdel-Hafez, M., & Alahmad, M. "Cognitive radio for smart grid with security considerations", *Computers*, vol. 5, no. 2, 2016.